iJETRM
International Journal of Engineering Technology Research & Management
Published By:
https://www.ijetrm.com/

INFLUENCE OF THERMO-DIFFUSION AND DIFFUSION-THERMO ON MHD HEAT MASS TRANSFER COUETTE FLOW IN THE PRESENCE BUOYANCY EFFECTS DUE TO RAMPED AND ISOTHERMAL TEMPERATURE

[1]F. Abdullah, [2]D. A. Sani and [3]I. H. Wala
[1,2]Department of Mathematics Waziri Umaru Fedral Polytechnic, Birnin Kebbi, Kebbi State
[3]Department of Statistics Waziri Umaru Fedral Polytechnic, Birnin Kebbi, Kebbi State
farukabdullahi@wufpbk.edu.ng

ABSTRACT
Numerical study was conducted to examine the impacts of Soret and Dufour on MHD Couette flow heat mass transfer free-convection in vertical channels under the influence of buoyancy distribution effects due to the ramped and isothermal temperature. The coupled non-linear dimensional governing partial differential equations and their initials and boundary conditions of the flow were changed to dimensionless form using appropriate dimensionless quantities. Finite element method was applied in finding the numerical solutions of the time-dependent momentum, energy and concentration equations subject to initial and boundary conditions. The expressions of velocity, temperature, concentration, skin friction, Nusselt number as well as Sherwood were obtained numerically subject to ramped and isothermal temperature. Some selected set graphical results showing the influence of controlling parameters involved in the flow formation were discussed using line graphs. From the results shown it was seen that rise of Ratio of Mass Transfer Parameter N, Porosity Parameter K, Buoyancy Parameter r_t , Eckert Number Ec and Dufour Number enhances velocity profile, while the reverse is the case for the increase of Magnetic Field Parameter M and Prandlt Number Pr. Correspondingly, rise in Ratio of Mass Transfer Parameter, Porosity Parameter K, Buoyancy Parameter r_t , Eckert Number Ec boosts temperature profile and diminishes it with rise in Prandlt Number Pr. Furthermore, concentration profile gets increased with the increase of Schmidt Number Sc. At y=0, the Skin friction diminishes with the increase of Soret number (Sr) and enhances with the increase in Dufour number (Df). Also, at y=0, the Nusselt Number gets enlarged with the increase of Soret number (Sr) and gets diminished with the increase in Dufour number (Df)

Keywords:
MHD, Dufour effect, Buoyancy distribution effect, Heat Mass Transfer

1 INTRODUCTION

Studying the of combined influence of heat and mass transfer is very vital in understanding some technical transfer processes (Siva et al., 2016). Applications of heat and mass transfer simultaneously are usually seen in chemical processing industries like polymer production industries and food processing industries. Apart from mass flux that is generated by the temperature gradient, there is also an energy flux which is generated by composition gradient. Temperature gradients creates mass flux and this mass flux is known as soret or thermo-diffusion effect. On the other hand, an energy flux that composition gradient creates is known Dufour or diffusion-thermo. Because of how important thermo-diffusion and diffusion-thermo have, in a fluid with very light molecular weight and medium molecular weight, that is why many researchers have turned their attention in studying these types of flows.

Chandra and Raju (2018) studied the influence of Soret and Dufour on heat and mass transfer unsteady MHD natural convection in porous medium in the presences of variable temperature and concentration. Likewise, Reddy et al., (2018) examined the impact of MHD unsteady viscous incompressible fluid in a semi-infinite inclined permeable moving plate in the presence of Soret and Dufour. The analyzation of the influence of mixed convection of Oldroyd was carried out by (Bilal et al., 2016). The influence of thermo-diffusion and diffusion-thermo on MHD

iJETRM
International Journal of Engineering Technology Research & Management
Published By:
https://www.ijetrm.com/

heat and mass transfer in a porous vertical surface was carried out by (Emmanuel et al., 2015) and reported that both Soret and Dufour boosts heat and mass transfer. Furthermore, Sasikumar and Govidarajan (2018) analyzed the impact of thermo-diffusion on MHD oscillatory flow under the influence of chemical reaction and reported the velocity profile gets enhanced with the increase of soret number. Moreover, Gbadeyan (2018) studied effects of Soret and Dufour MHD heat mass transfer free-convective in an infinite vertical channels under the influence of chemical reaction and discovered that velocity profile gets reduced with increase of Dufour and Soret number. The investigations of Soret and Dufour MHD heat and mass transfer of viscoelastic fluid in a semi-vertical channel was carried out by Idowu and Falodun (2019) and revealed that temperature profile gets enhanced with the increase of Dufour number and also velocity and concentration profile get enhanced with the increase of Soret number.

The influence of MHD unsteady natural convection couette flow of an electrically conducting water in the presence ramped and isothermal temperature was studied by Reddy et al., (2017). Also, Shankar and Rajashekar (2016) examined the effects of Soret, chemical reaction and radiation on MHD heat mass transfer flow in porous medium and discovered that increase in soret number increases velocity and concentration profile. The analyzation of thermo-diffusion on MHD heat and mass transfer free-convective porous medium in the presence of heat source and thermal radiation was carried out by Geethan et al., (2016) and revealed that soret number increases velocity profile and skin friction. Furthermore, Shankar and Rashekar (2017) analyzed the impact of MHD viscous dissipation, and thermo-diffusion on unsteady heat and mass transfer and discovered that velocity profile decreases with the increase in Dufour number and phase angle. The influence of Dufour, radiation absorption chemical reaction and viscous dissipation on MHD unsteady heat and mass transfer free-convective casson fluid in a semi-infinite vertical oscillatory porous plate was carried out by Rajakumar et al., (2018). This study was built up from the research of Prabhakar (2016) in which he investigated the influence of MHD viscous dissipation heat and mass transfer free-convective vertical channels under the uniform influence magnetic field. The study adopted and extended the Prabhakar (2016) model by incorporating buoyancy distribution parameter, thermo-diffusion and diffussion-thermo on MHD unsteady heat and mass transfer couette flow in the presence of ramped and isothermal temperature. Furthermore, the study used finite element method (FEM) in finding the numerical solution coupled non-linear governing partial differential equations. The expression of velocity, temperature and concentration were obtained numerically and discussed using line graphs.

2 FORMULATION OF THE PROBLEM

Consider a time-dependent heat and mass transfer free-convective couette flow of an incompressible electrically conducting fluid in a finite vertical plate.

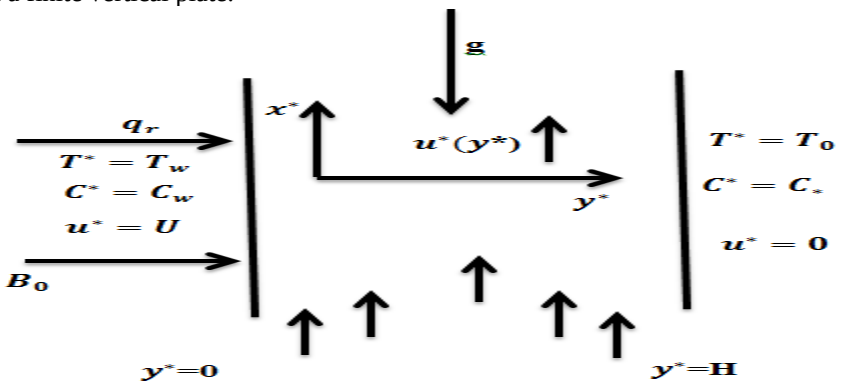

Figure 1: Geometry of the Problem

Assume the x*-axis be taken along the plate in the vertically upward direction and the and the y* axis is taken normal to the plate normal. There is has been uniform magnetic field of intensity H_0 which is applied transversely to the plate transversely. The temperature of the plate T^* and the fluid T_w^* are taken to be the same. The concentration of species at the plate C_w^* and C_0^* are assumed to be the same. When time t*>0, the plate is changed to T_w^*, which is then maintained constant thereby leading to the convection current to flow close to the plate and mass is applied at a constant rate. Under these conditions the flow variables are at a constant function of time and space (channel width)

iJETRM
International Journal of Engineering Technology Research & Management
Published By:
https://www.ijetrm.com/

y* alone. By using Boussineq approximation the governing equations describing velocity, temperature and concentration in the presence of soret, Dufour and other controlling parameters of the three problems take the following form:

Velocity equation

$$\frac{\partial u^*}{\partial t^*} = \frac{\partial^2 u^*}{\partial y^{*2}} + g\beta(T^* - T_w^*) - g\beta^{\bullet}(C^* - C_0) - \frac{\sigma\mu_e{}^2 H_0{}^2 u^*}{\rho} - \frac{\nu u^*}{K^*} \quad (2.1)$$

Temperature equation

$$\rho C_p \frac{\partial T^*}{\partial t^*} = k\frac{\partial^2 T^*}{\partial y^{*2}} + \mu\left[\frac{\partial u^*}{\partial y^*}\right]^2 + \frac{D_m \partial^2 C^*}{\alpha \partial y^{*2}} \quad (2.2)$$

Concertation equation

$$\frac{\partial C^*}{\partial t^*} = \frac{\partial^2 C^*}{\partial y^{*2}} + \frac{S_t \partial^2 \theta^*}{\alpha \partial y^{*2}} \quad (2.3)$$

The initial and boundary conditions of the problems are:

Case I: Isothermal Temperature **Case II: Continuous Ramped Temperature**

$$\left.\begin{array}{l} t^* \le 0,\ u^* = 0,\ T^* = T_0 \ \text{for all}\ 0 \le y^* \le L \\ t^* > 0 \left\{ \begin{array}{l} u^* = u,\ T^* = T_w,\ C^* = C_w^* \ \text{at}\ y^* = 0 \\ u^* = 0, T^* = r_t^* T,\ C^* = C_w^* \ \text{at}\ y^* = L \end{array}\right. \end{array}\right\} \qquad \left.\begin{array}{l} t^* \le 0,\ u^* = 0,\ T^* = T_0 \ \text{for all}\ 0 \le y^* \le L \\ t^* > 0 \left\{ \begin{array}{l} u^* = u,\ T^* = T_0 + \dfrac{(T_w^* - T_0)t^*}{T_R},\ C^* = C_w^* \ \text{at}\ y^* = 0 \\ u^* = 0, T^* = r_t^* T,\ C^* = C_w^* \ \text{at}\ y^* = L \end{array}\right. \end{array}\right\} \quad (2.4)$$

The non- dimensional quantities introduced in the above equations are defined as:

$$\left.\begin{array}{llll} U_0 = (\nu g\beta\Delta T)^{1/3}, & \mathrm{L} = \left(\dfrac{g\beta\Delta T}{\nu^2}\right)^{-1/3} & \mathrm{T}_R = \dfrac{(g\beta\Delta T)^{-2/3}}{\nu^{-1/3}} & \\ \Delta T = T_w^* - T_0^*, & \mathrm{t} = \dfrac{t^*}{T_R}, & \mathrm{y} = \dfrac{y^*}{L}, & \mathrm{r_t} = \dfrac{r_t^* - T_0}{T_w^* - T_0} \\ u = \dfrac{u^*}{U_0}, & \mathrm{K} = \dfrac{K^*}{\nu T_R}, & \theta = \dfrac{T^* - T_0}{T_w^* - T_0}, & \phi = \dfrac{C^* - C_0}{C_w^* - C_0} \\ \mathrm{Pr} = \dfrac{\mu C_P}{k}, & \mathrm{Sc} = \dfrac{\nu}{D_m}, & Ec = \dfrac{U_0^2}{C_P \Delta T}, & \mathrm{Sr} = \dfrac{S_t(T_w - T_0)}{\alpha(C_w - C_0)} \\ N = \dfrac{\beta^{\bullet}(C_w^* - C_\infty^*)}{\beta(T_W^* - T_0^*)}, & M = \dfrac{\sigma\mu_0^2 H_0^2 T_R}{\rho} & \mathrm{Df} = \dfrac{D_m(C_w - C_0)}{\alpha(T_w - T_0)} & \end{array}\right\} \quad (2.5)$$

3 Method of the Solution

The method applied to find the numerical solutions of our coupled non-linear partial differential equations was finite element (Galerkin's approach).

Now applying (2.5) Now on (2.5) into (2.1) - (2.4), the following dimensionless governing partial differential equations were gotten:

iJETRM
International Journal of Engineering Technology Research & Management
Published By:
https://www.ijetrm.com/

$$\frac{\P u}{\P t} = \frac{\P^2 u}{\P y^2} + Grq + Nf - (M + \frac{1}{K})u \quad (3.1)$$

$$Pr\frac{\partial \theta}{\partial t} = \frac{\partial^2 \theta}{\partial y^2} + Ec\left(\frac{\partial u}{\partial y}\right)^2 + Df\frac{\partial^2 \phi}{\partial^2 y^2} \quad (3.2)$$

$$Sc\frac{\partial \phi}{\partial t} = \frac{\partial^2 \phi}{\partial y^2} + S_r\frac{\partial^2 \theta}{\partial y^2} \quad (3.3)$$

Case I: Isothermal Temperature **Case II: Continuous Ramped Temperature**

$$\left.\begin{array}{l} t \le 0,\ u = 0, \theta = 0, \phi = 0 \ \ for \ \ all \ \ y \\ For\ t \ge 0: \\ u = 1, \theta = 1, \phi = 1 \quad at \ \ y = 0 \\ u = 0, \theta = \mathrm{r}_t, \phi = 0 \quad at \ \ y = 1 \end{array}\right\} \qquad \left.\begin{array}{l} t \le 0,\ u = 0, \theta = 0, \phi = 0 \ \ for \ \ all \ \ y \\ For\ t \ge 0: \\ u = 1, \theta = t, \phi = 1 \quad at \ \ y = 0 \\ u = 0, \theta = \mathrm{r}_t, \phi = 0 \quad at \ \ y = 1 \end{array}\right\} \quad (3.4)$$

Now (3.1) solving under the boundary conditions (3.4) using above mentioned method over the element ℓ, $y_i \le y \le y_j$

$$\int_{y_i}^{y_j}\left\{N^T\left[\frac{\partial^2 u}{\partial y^2} - \frac{\partial u}{\partial t} - u(M + \frac{1}{K}) + Nf + q\right]\right\}dy = 0 \quad (3.4)$$

Equation (3.4) is reduce to

$$\int_{y_i}^{y_j}\left\{N^T\left[\frac{\partial^2 u}{\partial y^2} - \frac{\partial u}{\partial t} - M_1 u + P\right]\right\}dy = 0 \quad (3.5)$$

Where $M_1 = M + \frac{1}{K}$ and $P = \theta + N\phi$

Applying integration by part to equation (3.5) yield;

$$[N^T\frac{\P u}{\P t}]_{y_i}^{yj} - \int_{y_i}^{y_i}\frac{\P N^T}{\P y}\frac{\P u}{\P y}dy - \int_{y_i}^{y_i}N^T\frac{\P u}{\P t}dy - M_1\int_{y_i}^{y_i}N^T u dy + P\int_{y_i}^{y_i}N^T dy = 0 \quad (3.6)$$

Neglecting the first term of equation (3.6)

$$\int_{y_i}^{y_i}\frac{\P N^T}{\P y}\frac{\P u}{\P y}dy + \int_{y_i}^{y_i}N^T\frac{\P u}{\P t}dy + M_1\int_{y_i}^{y_i}N^T u dy - P\int_{y_i}^{y_i}N^T dy = 0 \quad (3.7)$$

We let $u^{(e)} = u_i N_i + u_j N_j \Rightarrow u^{(e)} = [N][u]^T$ be the linear approximation solution over the two nodal element e, $(y_i \le y \le y_j)$ where $u^{(e)} = [u_i\ u_j]$, $N = [N_i N_j]$ also u_i *and* u_j are the velocity component at the i^{th} and j^{th} nodes of the typical element (e) $(y_i \le y \le y_j)$ furthermore, N_i and N_j are basis (or shape) functions defined as follows:

iJETRM
International Journal of Engineering Technology Research & Management
Published By:
https://www.ijetrm.com/

$$N_i = \frac{y_j - y}{y_j - y_i},\ N_j = \frac{y - y_i}{y_j - y_i}$$

Hence equation (3.7) take the form

$$\int_{y_i}^{y_j}\begin{bmatrix} N_i'N_i' & N_i'N_j' \\ N_i'N_j' & N_j'N_j' \end{bmatrix}\begin{bmatrix} u_i \\ u_j \end{bmatrix}dy + \int_{y_i}^{y_j}\begin{bmatrix} N_iN_i & N_iN_j \\ N_iN_j & N_jN_j \end{bmatrix}\begin{bmatrix} \dot{u}_i \\ \dot{u}_j \end{bmatrix}dy + M_1\int_{y_i}^{y_j}\begin{bmatrix} N_iN_i & N_iN_j \\ N_iN_j & N_jN_j \end{bmatrix}\begin{bmatrix} u_i \\ u_j \end{bmatrix}dy - P\int_{y_i}^{y_j}\begin{bmatrix} N_i \\ N_j \end{bmatrix}dy = 0 \quad (3.8)$$

Simplifying of equation (3.8) gives:

$$\frac{1}{l}\begin{bmatrix} 1 & -1 \\ -1 & 1 \end{bmatrix}\begin{bmatrix} u_i \\ u_j \end{bmatrix} + \frac{l}{6}\begin{bmatrix} 2 & 1 \\ 1 & 2 \end{bmatrix}\begin{bmatrix} \dot{u}_i \\ \dot{u}_j \end{bmatrix} + \frac{M_1 l}{6}\begin{bmatrix} 2 & 1 \\ 1 & 2 \end{bmatrix}\begin{bmatrix} u_i \\ u_j \end{bmatrix} - \frac{lP}{2}\begin{bmatrix} 1 \\ 1 \end{bmatrix} = 0 \quad (3.9)$$

Here $l = y_j - y_i = h$ and prime and dot represent differentiation with respect to x and y respectively. Assembling the equations for the consecutive elements $y_{i-1} \le y \le y_i$ and $y_i \le y \le y_{i+1}$ the following are gotten:

$$\frac{1}{l^2}\begin{bmatrix} 1 & -1 & 0 \\ -1 & 2 & -1 \\ 0 & -1 & 1 \end{bmatrix}\begin{bmatrix} u_{i-1} \\ u_i \\ u_{i+1} \end{bmatrix} + \frac{1}{6}\begin{bmatrix} 2 & 1 & 0 \\ 1 & 4 & 1 \\ 0 & 1 & 2 \end{bmatrix}\begin{bmatrix} \dot{u}_{i-1} \\ \dot{u}_i \\ \dot{u}_{i+1} \end{bmatrix} + \frac{M}{6}\begin{bmatrix} 2 & 1 & 0 \\ 1 & 4 & 1 \\ 0 & 1 & 2 \end{bmatrix}\begin{bmatrix} u_{i-1} \\ u_i \\ u_{i+1} \end{bmatrix} - \frac{P}{2}\begin{bmatrix} 1 \\ 2 \\ 1 \end{bmatrix} \quad (3.10)$$

Considering the row corresponding to the node i to zero with $l = h$, from equation(3.10) the difference schemes reads

$$\frac{1}{h^2}(-u_{i-1} + 2u_i - u_{i+1}) + \frac{1}{6}(-\dot{u}_{i-1} + 4\dot{u}_i + \dot{u}_{i+1}) \frac{M_1}{6}(u_{i-1} + 4u_i + u_{i+1}) = P \quad (3.11)$$

Application of trapezoidal rule on (3.11) the following system in Crank-Nicolson are obtained

$$A_1u_{i-1}^{n+1} + A_2u_i^{n+1} + A_3u_{i+1}^{n+1} = A_4u_{i-1}^{n} + A_5u_i^{n} + A_6u_{i+1}^{n} + P^* \quad (3.12)$$

Also, solving (2.2) and (2.3) in the same way we have:

$$B_1q_{i-1}^{n+1} + B_2q_i^{n+1} + B_3q_{i+1}^{n+1} = B_4q_{i-1}^{n} + B_5q_i^{n} + B_6q_{i+1}^{n} + Q^* \quad (3.13)$$

$$C_1\phi_{i-1}^{n+1} + C_2\phi_i^{n+1} + C_3\phi_{i+1}^{n+1} = C_4\phi_{i-1}^{n} + C_5\phi_i^{n} + C_6\phi_{i+1}^{n} + R^* = 0 \quad (3.14)$$

Where

iJETRM
International Journal of Engineering Technology Research & Management
Published By:
https://www.ijetrm.com/

$A_1 = 2-6r+rM_1h^2, \quad A_2 = 8+12r+rM_1h^2, \quad A_3 = 2-6r+rM_1h^2$

$A_4 = 2+6r-rM_1h^2, \quad A_5 = 8-12r-4rrM_1h^2, \quad A_6 = 2+6r-rM_1h^2$

$$P^* = 12rh^2(\theta_i^n + N\phi_i^n)$$

$B_1 = Pr-3r, \quad B_2 = 4Pr+6r\ , \quad B_3 = Pr-3r$

$B_4 = Pr+3r, \quad B_5 = 4Pr-6r, \quad B_6 = Pr+3r$

$$Q^* = 6r\,Pr\,Ec\left[\left[\frac{\partial u}{\partial y}\right]^2 + \frac{\partial^2\phi}{\partial^2 y}\right]$$

$C_1 = Pr-3r, \quad C_2 = 4Pr+6r\ , \quad C_3 = Pr-3r$

$C_4 = Pr+3r, \quad C_5 = 4Pr-6r, \quad C_6 = Pr+3r$

$$R^* = 6h^2 ScSr\frac{\partial^2\theta}{\partial y^2}$$

Here $r = \frac{k}{h^2}$ and h and k are mesh size along y direction and time direction. Index i refers to space and j refers to the time refers to. In equations (3.2), (3.13) and (3.44), taking $i = 1(1)n$ and using the initial and boundary conditions (3.4), the following system of equations is obtained

$$A_i X_i = B_i \qquad i = 1(1)n$$

Here A_i matrices of order n and X_i and B_i are column matrices with n components. The solution of the system of the equations were obtained by applying Thomas algorithm for velocity, temperature and concentration. The results of various parameters are computed and presented graphically. The skin friction, Nusselt number and Sherwood number are vital physical parameters for this type boundary layer's flow, with known values of velocity, temperature and concentration fields.

The skin friction at the plate is given by in non-dimensional form as:

$$\tau = \left[\frac{\partial u}{\partial y}\right]_{y=0,y=1} \tag{3.15}$$

The rate of heat transfer coefficient can be calculated in terms of Nusselt number is given in dimensionless form as:

$$Nu = -\left[\frac{\partial \theta}{\partial y}\right]_{y=0,y=1} \tag{3.16}$$

The rate of mass transfer can be calculated in terms of Sherwood number in its dimensionless form as:

$$Sh = -\left[\frac{\partial \phi}{\partial y}\right]_{y=0,y=1} \tag{3.17}$$

4 RESULTS AND DICUSSION

In order to analyze the impact of various parameters on flow field boundary layer region. Finite element method was applied in solving non-dimensional governing partial differential equations (3.1) to (3.3) subject to initial and boundary conditions (3.4). We examined the effects of Prandlt number Pr, Soret number Sr, Dufour number Df, Eckert number Ec, Schmidt number Sc, Magnetic Field Parameter M, Porosity Parameter K, Buoyancy Parameter r_t and Ratio of mass transfer N. To capture real picture of the problem under discussion we have performed numerical computations using different values of magnetic parameter ($M = 2, M = 4, M = 6$), Prandtl number($Pr = 0.71, Pr = 3, Pr = 7$), Dufour number ($Df = 0.01, Df = 0.02, Df = 0.03$), Eckert number ($Ec = 0.03, Ec = 0.06, Ec = 0.09$) Schmidt number ($Sc = 2, Sc = 4, Sc = 6$), ratio of mass transformation ($N = 2, N = 4 = N = 6$), porosity parameter $K = 2, K = 4, K = 6$), Soret number ($Sr = 0.02, Sr = 0.04 = Sr = 0.06$) and the Buoyancy Parameter ($r_t = 2, r_{t=}4, r_{t=}6$) on fluid velocity, temperature and concentration were presented graphically

Velocity Profile

iJETRM
International Journal of Engineering Technology Research & Management
Published By:
https://www.ijetrm.com/

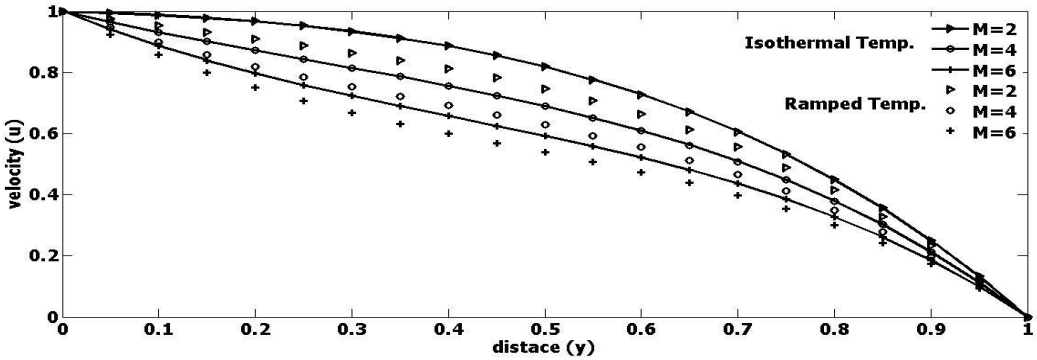

Figure 2: Effect of M on velocity profile

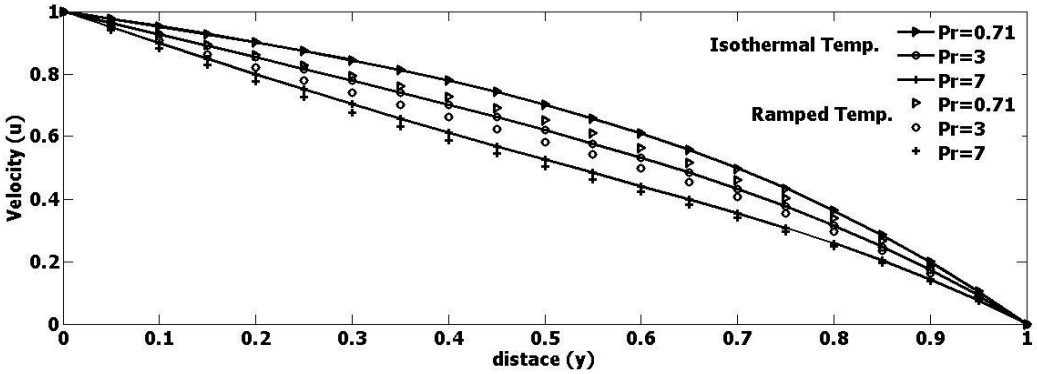

Figure 3: Effect of Pr on velocity profile

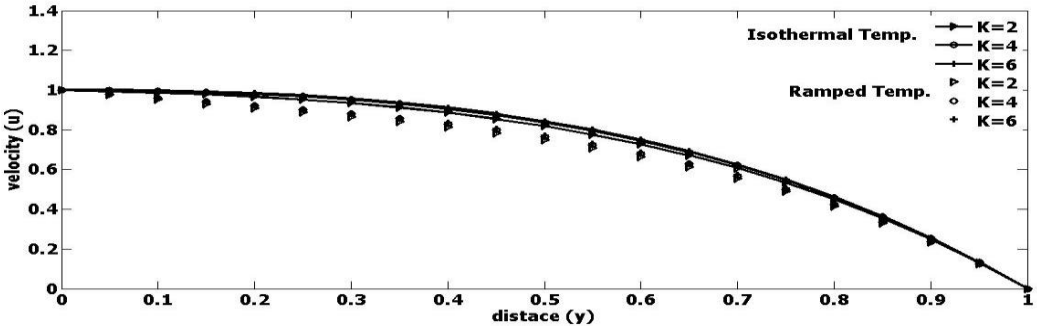

Figure 4: Effect of K on velocity profile

iJETRM
International Journal of Engineering Technology Research & Management
Published By:
https://www.ijetrm.com/

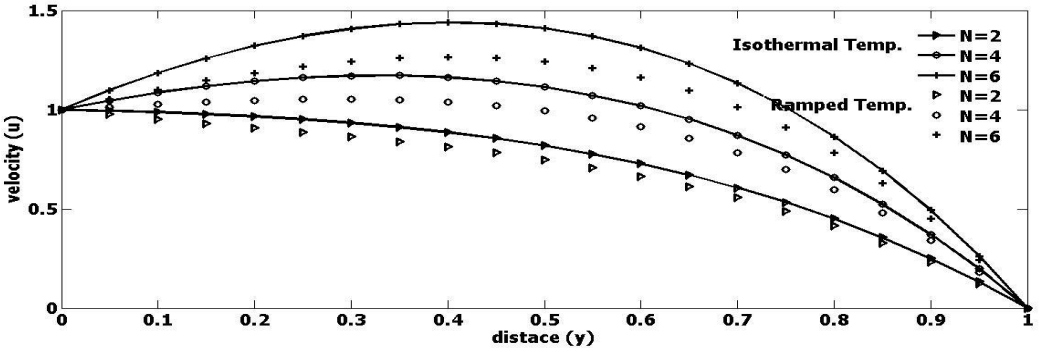

Figure 5: Effect of N on velocity profile

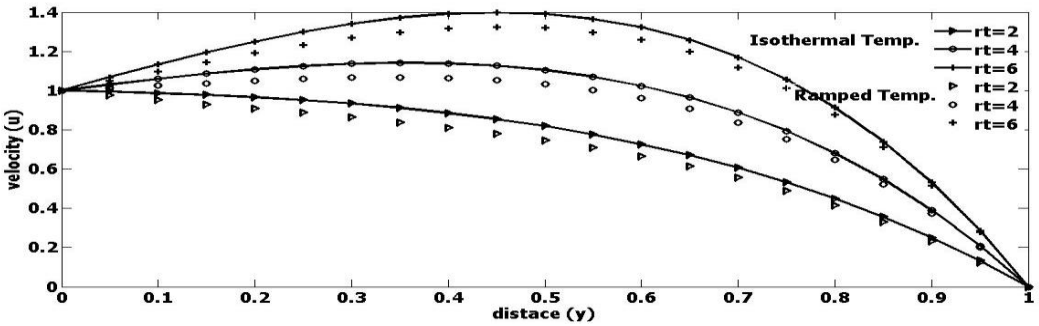

Figure 6: Effect of r_t on velocity profile

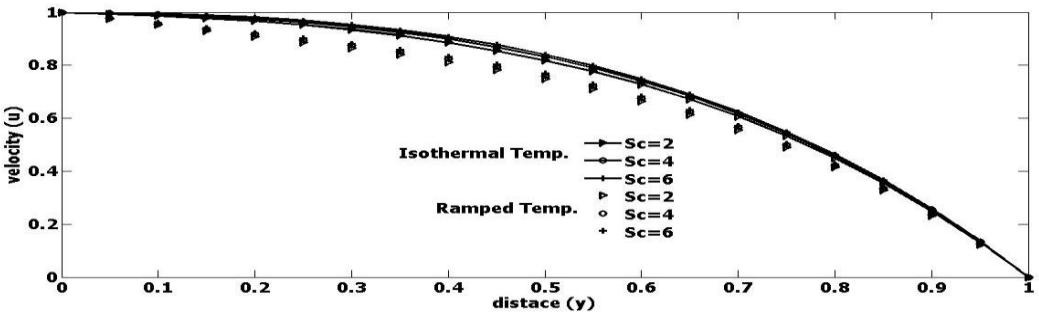

Figure 7: Effect of Sc on velocity profile

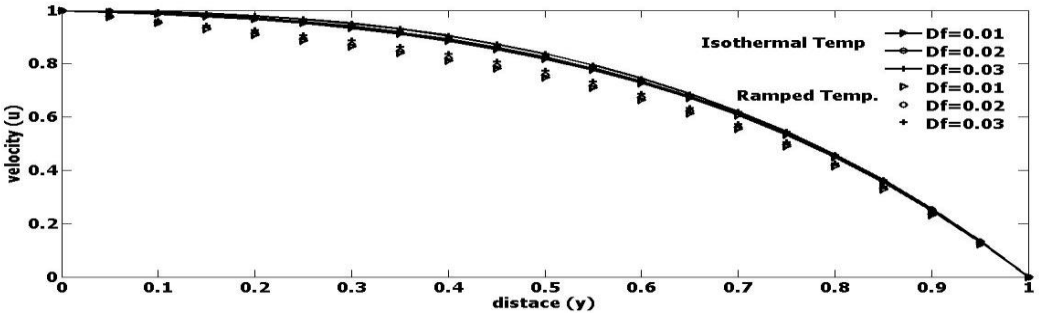

Figure 8: Effect of Df on velocity profile

iJETRM
International Journal of Engineering Technology Research & Management
Published By:
https://www.ijetrm.com/

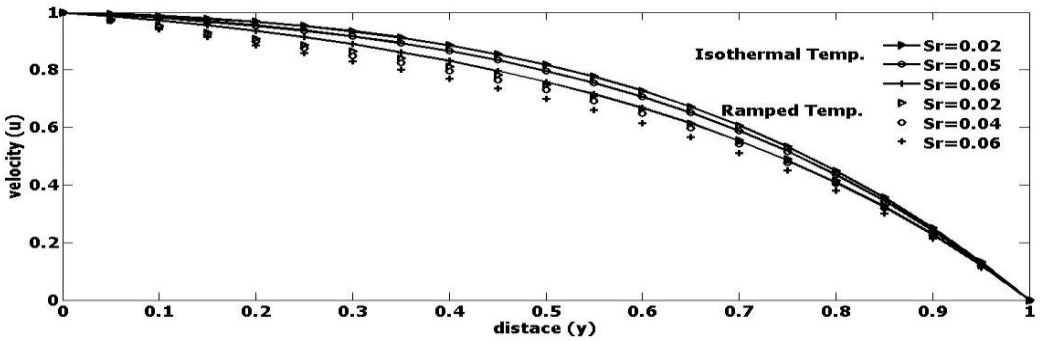

Figure 9: Effect of Sr on velocity profile

Figure 2&3 illustrate the behaviour of velocity profile for different values Magnetic Parameter (M) and Prandtl number (Pr) for both ramped and isothermal temperature. It is noticed that, the velocity profile gets reduced with the increase Magnetic Parameter and (M) Prandtl number (Pr). While opposite behavior is noticed in **Figure 4,5&6** with the porosity parameter (K), Ratio of Mass transfer (N) and Buoyancy parameter (r_t). Similarly, there is slight rise in velocity profile in **Figure 7&8** with the increase in Schmidt number (Sc) and Dufour number (Df) for both ramped and isothermal temperature. While opposite behavior is seen in **Figure 9** with the increase of Soret number (Sr)

Temperature Profiles

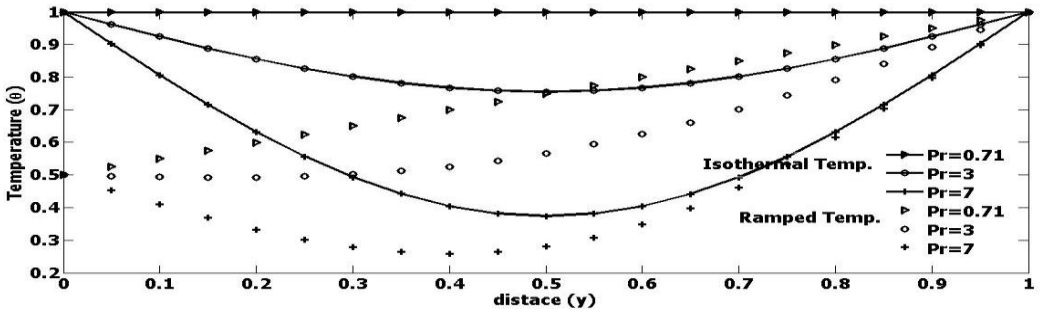

Figure 10: Effect Pr on temperature profile

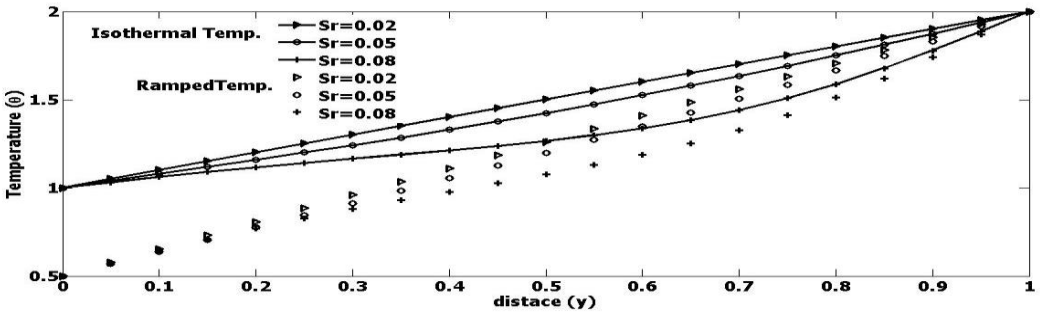

Figure 11: Effect Sr on temperature profile

iJETRM
International Journal of Engineering Technology Research & Management
Published By:
https://www.ijetrm.com/

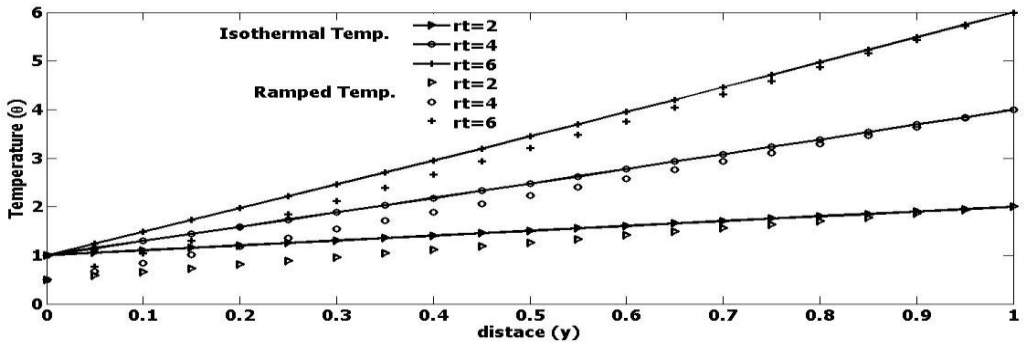

Figure 4.12: Effect r_t on temperature profile

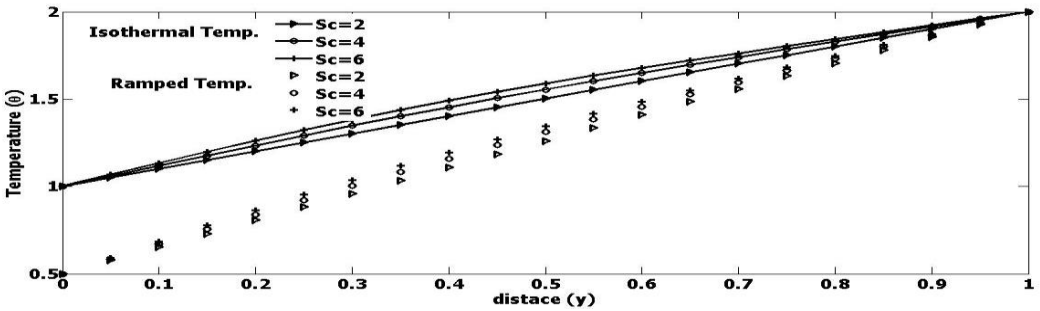

Figure 4.13: Effect Sc on tempera

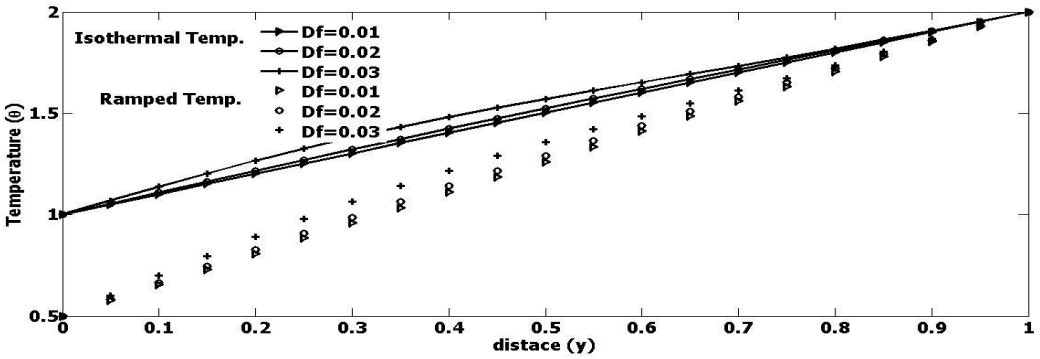

Figure 4.14: Effect Df on temperature profile

Figure 10&4.11 display the influence of Prandtl number (Pr) and Soret number (Sr) on temperature profile for both ramped and isothermal temperature. From the figure the temperature profile diminishes with the increase of Prandtl number (Pr) and Soret number (Sr. While opposite behavior is seen in **Figure 12,4.13, 4.14** with the increase in buoyancy parameter (r_t) and Schmidt number (Sc) and Dufour number (Df).

Concentration Profile

iJETRM
International Journal of Engineering Technology Research & Management
Published By:
https://www.ijetrm.com/

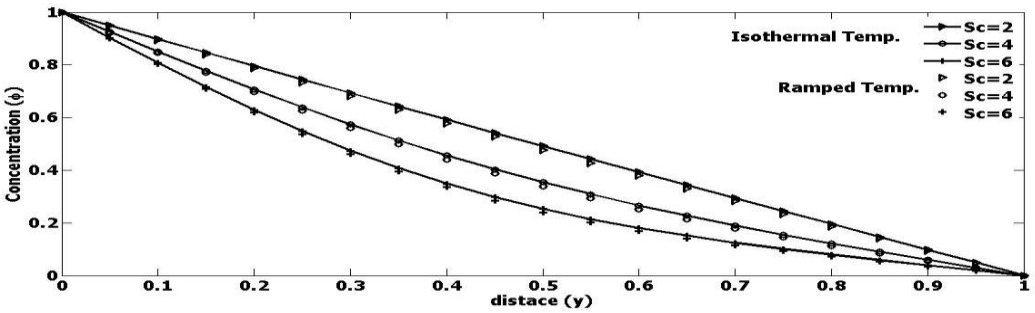

Figure 4.15: Effect Sc on Concentration profile

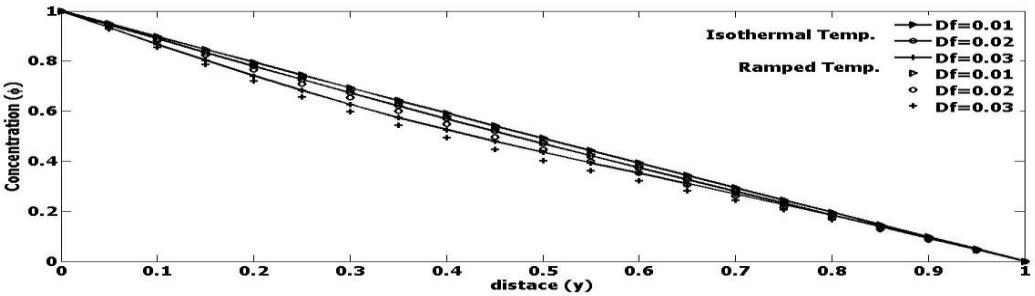

Figure 16: Effect of Df on Concentration profile

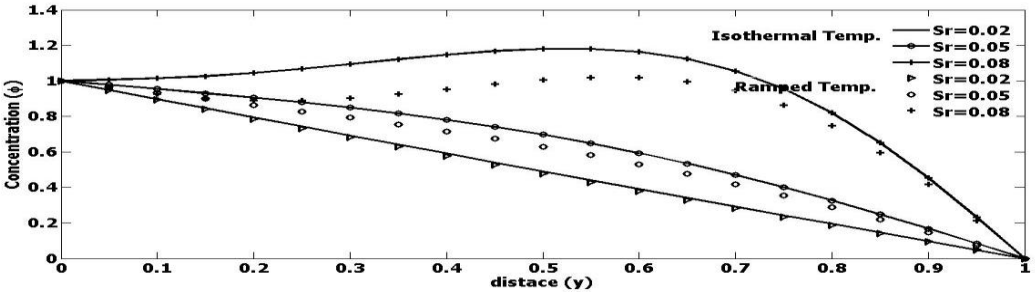

Figure 17: Effect Sr on temperature profile

Figure 15&16 show the impact of Schmidt number (Sc) and Dufour number (Df)on fluid concentration for both ramped and isothermal temperature. It is seen that the concentration profile gets diminished with the increase of both Schmidt number (Sc) and Dufour number (Df), Reverse is the case in **figure 17** with the increase of Soret number (Sc).

Skin Friction Profile

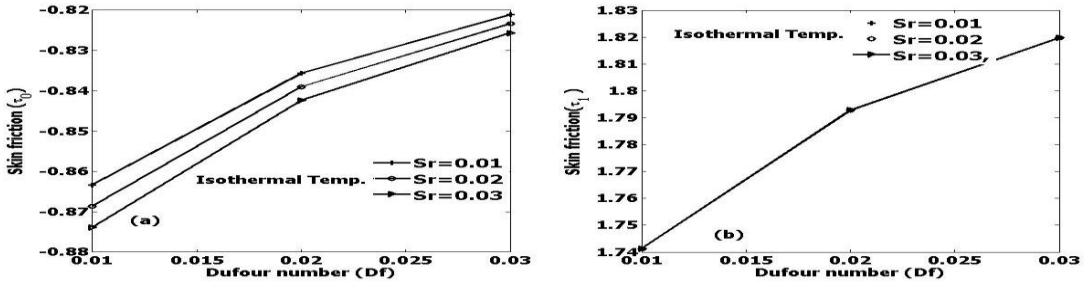

Figure 18: Effect of Sr and Df on skin friction due to isothermal temperature

iJETRM
International Journal of Engineering Technology Research & Management
Published By:
https://www.ijetrm.com/

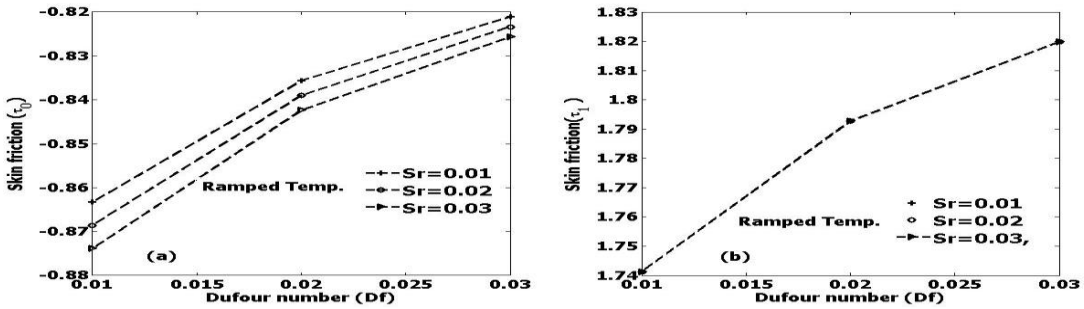

Figure 19: Effect of Sr and Df on skin friction due to ramped temperature

Figure 18&19 dipict the effect of Soret (Sr) and Dufour number (Df) on Skin friction for both ramped and isothermal temperature. The Skin friction diminishes in **figure 18(a) &19(a)** with the increase of Soret number (Sr) and enhances with the increase in Dufour number (Df). Additionally, no increase or decrease is observed in Skin friction in **figure 18(b) &4.19(b)** with the increase of Soret number (Sr) and it enhances with the increase in Dufour number (Df).

Nusselt Number Profile

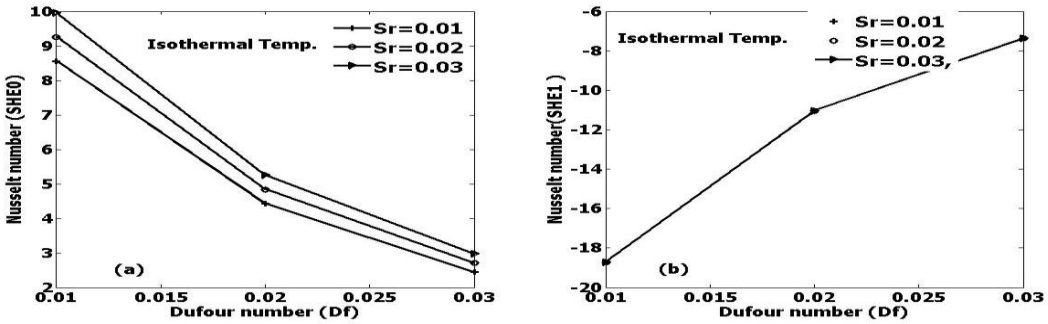

Figure 20: Effect of Sr and Df on Nusselt number due to isothermal temperature

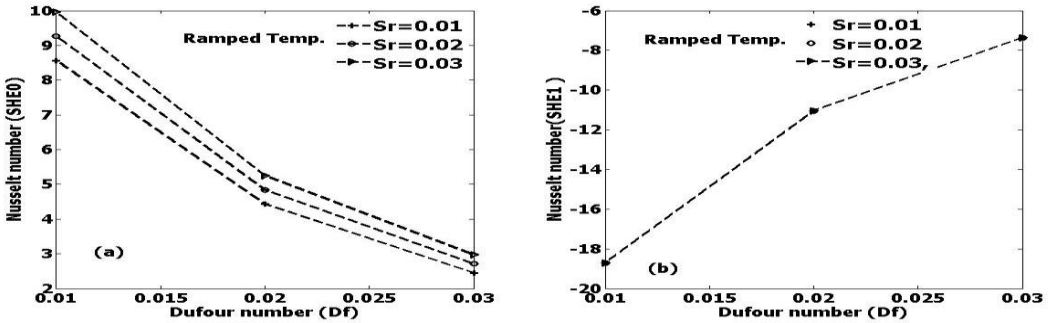

Figure 21: Effect of Sr and Df on Nusselt number due to ramped temperature

Figure 20&21 display the effect of Soret (Sr) and Dufour number (Df) on Nusselt Number for both ramped and isothermal temperature. The Nusselt Number gets enlarged in **figure 20(a) &21(a)** with the increase of Soret number (Sr) and gets diminished with the increase in Dufour number (Df). Additionally, no increase or decrease is observed in The Nusselt Number in **figure 20(b) &21(b)** with the increase of Soret number (Sr) and there is increase with the increase in Dufour number (Df).

Sherwood Number

iJETRM
International Journal of Engineering Technology Research & Management
Published By:
https://www.ijetrm.com/

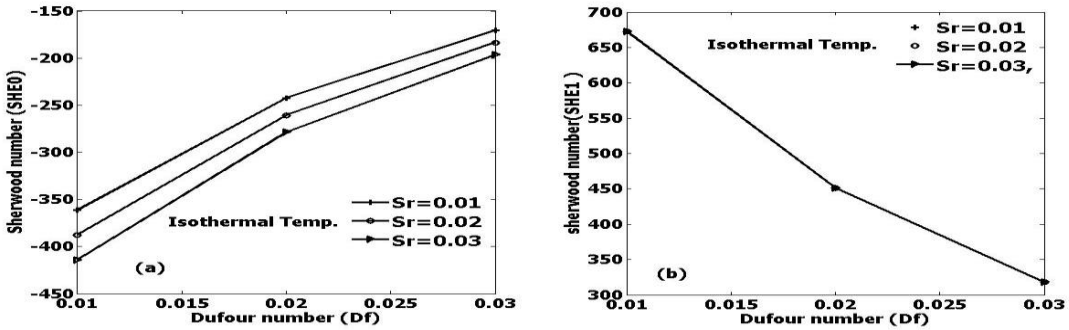

Figure 22: Effect of Sr and Df on Sherwood number due to isothermal temperature

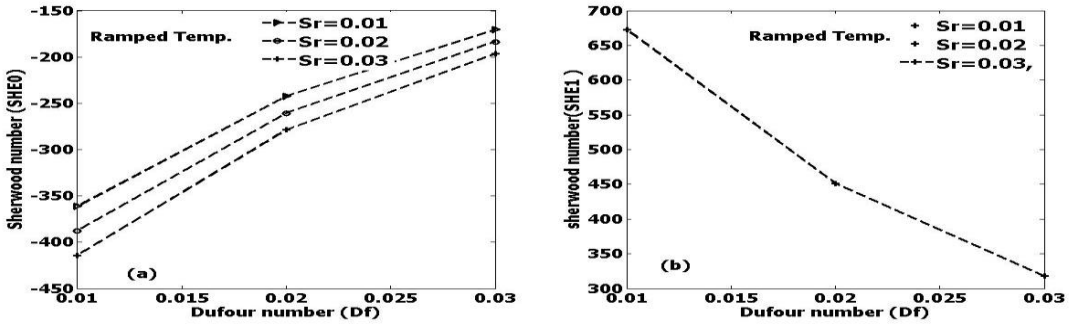

Figure 23: Effect of Sr and Df on Sherwood number due to ramped temperature

Figure 22&23 show the effect of Soret (Sr) and Dufour number (Df) on Sherwood Number for both ramped and isothermal temperature. The Sherwood Number gets enlarged in **figure 22(a) 23(a)** with the increase of both Soret number (Sr) and Dufour number (Df). Furthermore, no increase or decrease is observed in Sherwood Number in **figure 22(b)&4.23(b)** with the increase of Soret number (Sr) and it decreases with the increase in Dufour number (Df).

5 CONCLUSIONS

We analyzed the combined influence of Soret and Dufour on MHD unsteady heat and mass transfer coquette flow free-convective in the presence of buoyancy distributions effect due to ramped and isothermal temperature. From the outcome of study, the following conclusions were made:

i. The velocity profile is enlarged with the increase of, porosity parameter K, ratio of mass transfer parameter N, Schmidt number Sc, Dufour number Df and buoyancy effect term parameter r_t,. It decreases with increase of Magnetic parameter M, Soret number Sr and Prandtl number Pr

ii. The temperature profile gets increased with the increase of buoyancy effect parameter term r_t, Schmidt number Sc and Dufour Df. It decreases with increase of Prandtl number Pr and Soret number Sr.

iii. The concentration profile gets enhanced significantly with the increased of Soret number Sr. It decreases with increase of Schmidt number Sc and Dufour number Df.

iv. At y=0, the Skin friction diminishes with the increase of Soret number (Sr) and enhances with the increase in Dufour number (Df). It does not increase or decrease with the increase of Soret number (Sr) and it enhances with the increase in Dufour number (Df) at y=1.

v. At y=0, the Nusselt Number gets enlarged with the increase of Soret number (Sr) and gets diminished with the increase in Dufour number (Df). Additionally, it does not increase or decrease with the increase of Soret number (Sr) and increases with the increase in Dufour number (Df) at y=1.

iJETRM
International Journal of Engineering Technology Research & Management
Published By:
https://www.ijetrm.com/

vi. At y=0, the Sherwood Number gets enlarged with the increase of both Soret number (Sr) and Dufour number (Sr). It does not increase or decrease with the increase of Soret number (Sr) and it decreases with the increase in Dufour number (Df) at y=1.

REFFERENCES

A. S. Idowu, A.S., and Falodun, B.O. (2019). Soret–Dufour effects on MHD heat and mass transfer of Walter's-B viscoelastic fluid over a semi-infinite vertical plate: spectral relaxation analysis. *Journal of Taibah University for Science*. **13**(1) 49-62

Bilal, M. A., Hayat, T., Alsaedi, A., Shehzad, A.S. (2016). Soret and Dufour effects on the mixed convection flow of an Oldroyd-B fluid with convective boundary conditions. *Elsevier Journal*, **6** (2016), 917–924.

Chandra P. R., Raju M. C. & Raju, G. S. S. (2018). Magneto Hydrodynamic Convective Double Diffusive Laminar Boundary Layer Flow Past an Accelerated Vertical Plate. *International Journal of Engineering Research in Africa*; 20, 80-92.

Emmanuel, M. A., Yakubu, I. S., Daniel, G. A. (2015). Analytical Solution of Dufour and Soret Effects on Hydromagnetic Flow Past a Vertical Plate Embedded in a Porous Medium. *Advances in Physics Theories and Applications*, **44** (2015) 2225-0638

Gbadeyan, J.A., Oyekunlec, T.L., Fasogbon, P.F., and. Abubakar, J.U. (2018). Soret and Dufour effects on heat and mass transfer in chemically reacting MHD flow through a wavy channel. *Journal of Taibah University for Science*, **5**(12) 631–651

Geethan, S. K., Kiran, R. K., Vinod, G. K. & Varma, S. V. K. (2016). Soret and Radiation Effects on MHD Free Convection Slip Flow over an Inclined Porous Plate with Heat and Mass Flux. *Advanced Science Engineering and Medicine*; **8** (3), 1-10.

Prabhakar, R. B. (2016). Mass Transfer Effects on an Unsteady MHD Free Convective Flow of an Incompressible Viscous Dissipative Fluid Past an Infinite Vertical Porous Plate. *International Journal of Applied Mechanics and Engineering*; 21(1), 143-155.

Rajakumar, K. V. B., Balamurugan, K. S., Umasankara, R. M. & Ramana, V. (2018). Radiation, Dissipation and Dufour Effects on MHD Free Convection Casson Fluid Flow through a Vertical Oscillatory Porous Plate with Ion-Slip Current. *International Journal of Heat and Mass Transfer Technology;* **36** (2), 494-508.

Reddy, G. J., Raju, R. S., Rao, J. A. & Gorla, R. S. R. (2017). Unsteady MHD Heat Transfer in Couette Flow of Water at 4ºC in a Rotating System with Ramped Temperature via Finite Element Method. *International Journal of Applied Mechanics and Engineering;* **22**(1), 145-161.

Reddy, S.S., Vijayabhaskar, C. & Mahendar, D. (2018). Unsteady MHD Flow over an Inclined Porous Plate Embedded in Porous Medium with Heat Absorption and Soret-Dufour Effects. *International Journal of Pure and Applied Mathematics*; **120** (6), 8021-8049.

Sasikumar, J., and Govindarajan, A. (2019). Soret Effect on Chemically Radiating MHD Oscillatory Flow with Heat Source through Porous Medium in Asymmetric Wavy Channe. *National Conference on Mathematical Techniques and its Applications* **1000**(2018) 012034

Shankar, B. G. & Rajashekar, M. N. (2016). Finite Element Method Application of Effects on an Unsteady MHD Convective Heat and Mass Transfer Flow in a Semi-infinite Vertical Moving in a Porous Medium with Heat Source and Suction. *Journal of Mathematics;* **12** (6), 55-64.

Shankar, B. G. & Rajashekar, M. N. (2017), Finite Element Solution On Effects Of Viscous Dissipation & Diffusion Thermo On Unsteady MHD Flow Past An Impulsively Started Inclined Oscillating Plate With Mass Diffusion &Variable Temperature. *International Research Journal of Engineering and Technology;* **4** (2), 471-477

Siva, R. S. & Anjan, K. S. (2016). Finite Element Analysis of Heat and Mass Transfer past an Impulsively Moving Vertical Plate with Ramped Temperature. *Journal of Applied Science and Engineering*; **19** (4), 385-392.